

# Application of Stereocontrolled Stepwise [3+2] Cycloadditions to the Preparation of Inhibitors of $\alpha_4\beta_1$ -Integrin-Mediated Hepatic Melanoma Metastasis\*\*

Aizpea Zubia, Lorea Mendoza, Silvia Vivanco, Eneko Aldaba, Teresa Carrascal, Begoña Lecea, Ana Arrieta, Tahl Zimmerman, Fernando Vidal-Vanaclocha, and Fernando P. Cossío\*

Dedicated to Professor Cecilia Sarasola

Intravascular circulation of cancer cells represents a frequent event along neoplastic progression that seriously increases the probability of occurrence of metastasis. However, the adhesion of blood-borne cancer cells to the microvascular wall is a prerequisite for metastatic cell implantation at target organs. Similar to capillary homing of leukocytes, this process is proinflammatory cytokine-inducible and the mechanism involves specific binding between cancer and endothelial cell adhesion molecules.<sup>[1]</sup> Previously, we and others reported that integrin “very late antigen 4” (VLA-4,  $\alpha_4\beta_1$ ) accounts for melanoma cell adhesion to endothelium in metastasized organs.<sup>[2]</sup> As vascular adhesion cell molecule 1 (VCAM-1) is the natural ligand of VLA-4, the VLA-4–VCAM-1 interac-

[\*] Dr. A. Zubia, Dr. S. Vivanco, E. Aldaba, Prof. B. Lecea, Prof. A. Arrieta, Prof. F. P. Cossío

Facultad de Química-Kimika Fakultatea  
Universidad del País Vasco-Euskal Herriko Unibertsitatea  
P. O. Box 1072, 20080 San Sebastián-Donostia (Spain)  
Fax: (+34) 943-212-236  
E-mail: fpcossio@sq.ehu.es

Dr. L. Mendoza, Dr. T. Carrascal  
Dominion Pharmakine, Ltd.  
Zamudio Technology Park  
48170 Zamudio (Spain)

Prof. F. Vidal-Vanaclocha  
Facultad de Medicina y Odontología-Medikuntza eta Odontologia Fakultatea  
Universidad del País Vasco-Euskal Herriko Unibertsitatea  
48940 Lejona-Leioa (Spain)

T. Zimmerman  
Centro Nacional de Investigaciones Oncológicas (CNIO)  
Structural and Computational Biology Programme  
Melchor Fernández Almagro 3, 28029 Madrid (Spain)

[\*\*] This work was supported by the Universidad del País Vasco-Euskal Herriko Unibertsitatea, Gobierno Vasco-Eusko Jaurlaritza (grants 9/UPV00170.215-13548/2001 and -13641/2001), Dominion Pharmakine Ltd., and by the Spanish Ministerio de Educación y Ciencia (grants BQU2001-0904, BIO2003-02246, and SAF99-0042). A.Z. and E.A. are recipients of fellowships from the GV-EJ. We thank Dr. Francisco J. Blanco and Dr. Pascal García (CNIO, Spain) for their advice on the  $^{15}\text{N}$ – $^1\text{H}$  HSQC experiments. We also thank Dr. Antonio Llamas (Unidade de Raios X, Universidade de Santiago de Compostela, Spain) for the X-ray diffraction analysis of compound **11d**.



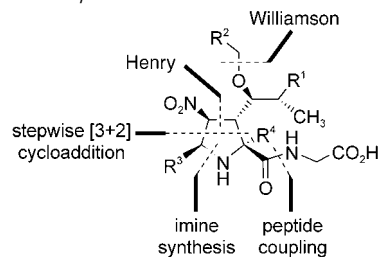
Supporting information for this article is available on the WWW under <http://www.angewandte.org> or from the author.

tion may, therefore, constitute an interesting molecular target for innovative therapy against melanoma dissemination. However, no results on the antimetastatic effects of synthetic VLA-4/VCAM-1 inhibitors have been reported to date, although interesting studies on synthetic inhibitors of the VLA-4/VCAM-1 interaction have been recently reported.<sup>[3]</sup> Herein, we demonstrate that small synthetic molecules which are designed to mimic the minimal requirements for binding between the natural macromolecules completely abrogate 1) melanoma cell adhesion to cytokine-activated endothelial cells and 2) melanoma cell responses to soluble and immobilized VCAM-1, and 3) efficiently inhibit metastatic development in vivo, without significantly affecting their cell viability, proliferation rate, or major metabolic activities.

Structural and electronic features of VCAM-1 were first examined in order to reproduce these features in the synthetic

inhibitors.<sup>[4]</sup> The crystal structure of domains 1 and 2 of VCAM-1 has been resolved by X-ray diffraction analysis.<sup>[5]</sup> Additionally, directed mutagenesis studies have determined that the CD loop in domain 1 of VCAM-1 is crucial for binding to VLA-4<sup>[5]</sup> (Figure 1 a). In the solvated molecule, the carboxymethyl group of Asp<sub>40</sub> has considerable conformational freedom and is surrounded by a relatively hydrophobic environment (Figure 1b). We reasoned that the compounds shown in Table 1 could mimic the structural and electronic

**Table 1:** General structure and retrosynthetic analysis of the novel inhibitors of the VLA-4/VCAM-1 interaction.



11	R <sup>1</sup>	R <sup>2</sup>	R <sup>3</sup> [a]	R <sup>4</sup>
a	Me	Ph	Ph	H
b	Me	Ph	<i>t</i> Bu	H
c	Me	2-FC <sub>6</sub> H <sub>4</sub>	Ph	H
d	Et	Ph	Ph	H
e	Me	2,6-F <sub>2</sub> C <sub>6</sub> H <sub>3</sub>	Ph	H
f	Et	Ph	<i>c</i> Hex	H
g	Et	3,5-F <sub>2</sub> C <sub>6</sub> H <sub>3</sub>	Ph	H
h	Et	Ph	<i>c</i> Pr	H
i	Et	2,3-F <sub>2</sub> C <sub>6</sub> H <sub>3</sub>	Ph	H
j	Et	Ph	Ph	Me
k	Et	Ph		H

[a] *c*Hex = cyclohexyl, *c*Pr = cyclopropyl, Bn = benzyl.

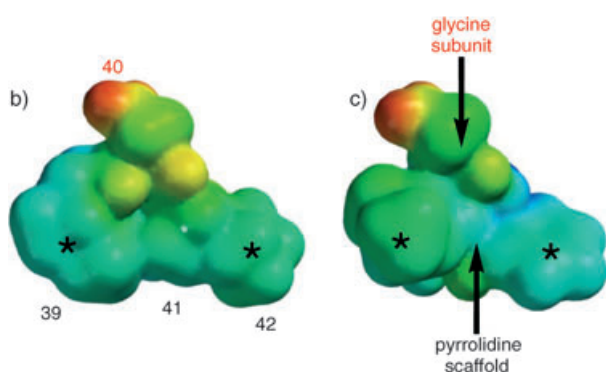
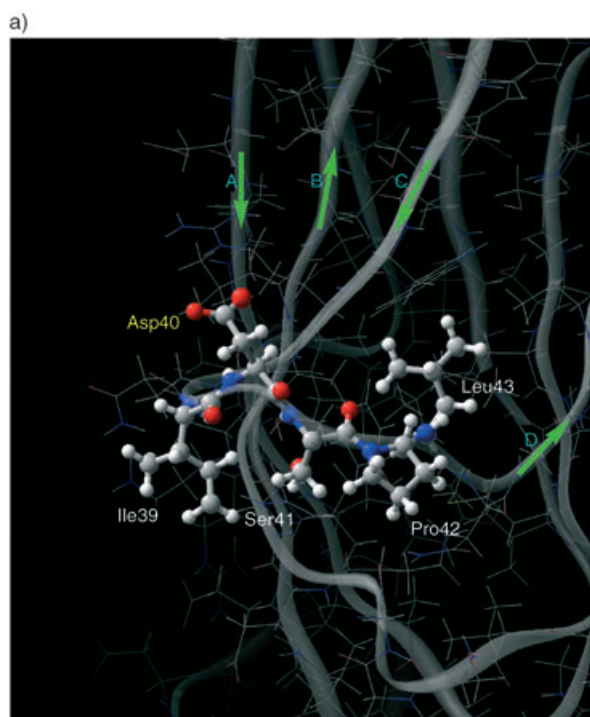
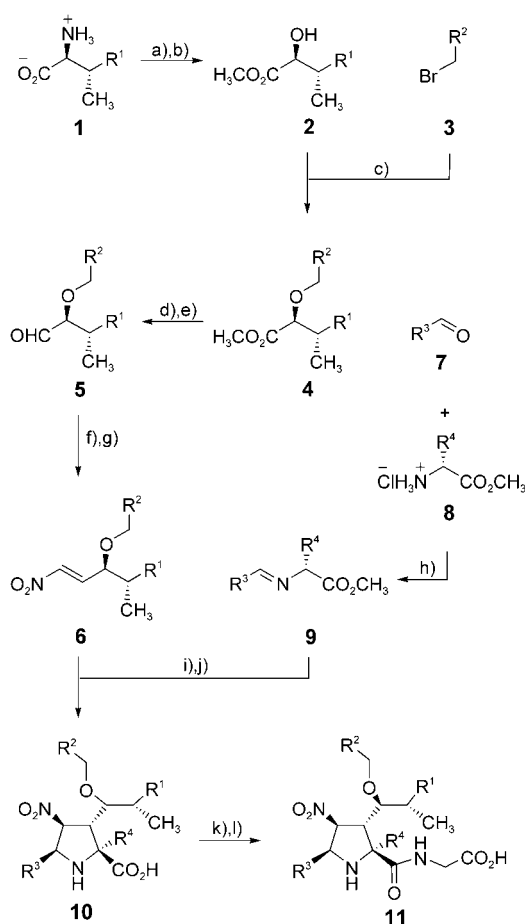


**Figure 1.** a) X-ray crystal structure (taken from ref. [5]) of the active loop of VCAM-1 which is involved in binding with integrin VLA-4. b), c) Electrostatic potential projected onto the electron density of the Ile39-Asp40-Ser41-Pro42 tetramer (b) and inhibitor **11d** (c); energies range from  $-138.2$  (red) to  $+100.2$  kcal mol<sup>-1</sup> (blue); asterisks (\*) indicate the hydrophobic regions in both structures.

features of the Ile39-Asp40-Ser41-Pro42 sequence of domain 1 of VCAM-1 (Figure 1c). Thus, the carboxymethyl-amido chain of these novel compounds reproduces the binding ability of Asp<sub>40</sub>, whereas the remaining groups provide the environment required for simulating the structural and electrostatic features of the remaining residues. Furthermore, the pyrrolidine ring confers the necessary restriction of conformational freedom to the molecule to mimic the energetically available conformations of the CD loop in the  $\beta$  barrel of domain 1 of VCAM-1 (Figure 1b and c). Therefore, these unnatural highly substituted pyrrolidine rings should bind to VLA-4 to disrupt VLA-4/VCAM-1-interaction-dependent mechanisms.

The new compounds **11** were synthesized in 12 preparative steps according to the design depicted in Table 1 and Scheme 1 (for more details, see Supporting Information). The starting materials were readily accessible and inexpensive chemicals such as *L*- $\alpha$ -amino acids (glycine, alanine, valine, and leucine), halides **3**, and aldehydes **7**. The key step in the synthetic route shown in Scheme 1 is the formal [3+2] cycloaddition between *E*-nitroalkenes **6** and imines **9** to yield pyrrolidines **10**. This reaction takes place with complete

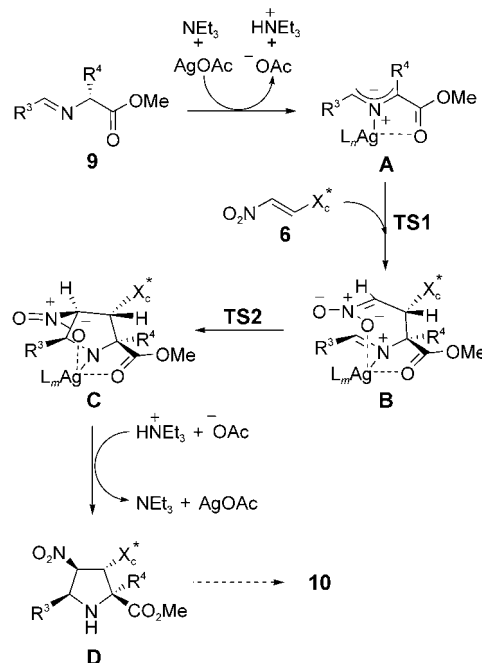


**Scheme 1.** Synthesis of compounds **11**. a) **1** (1.0 equiv in 1 N H<sub>2</sub>SO<sub>4</sub>), NaNO<sub>2</sub> (1.5 equiv in H<sub>2</sub>O), 0°C, 24 h, 83–90%; b) DMP (1.0 equiv), TsOH·H<sub>2</sub>O (0.007 equiv), MeOH, 45°C, 24 h, 88–96%; c) **2** (1.0 equiv), NaH (1.0 equiv), anhydrous THF/DMF (2:0.6), 0°C, 10 min, then **3** (1.2 equiv), RT, 24 h, 45–64%; d) LiAlH<sub>4</sub> (1.0 equiv), Et<sub>2</sub>O, 0°C, then **4** (1.0 equiv), Et<sub>2</sub>O, RT, 3 h, 80–90%; e) ClCOCOCl (1.5 equiv), DMSO (2.0 equiv), TEA (4.0 equiv), CH<sub>2</sub>Cl<sub>2</sub>, –67°C, 5 h, 79–90%; f) **5** (1.0 equiv), CH<sub>3</sub>NO<sub>2</sub> (5.0 equiv), TEA (0.14 equiv), RT, overnight, 87–96%; g) MsCl (1.2 equiv), DIPEA (2.5 equiv), CH<sub>2</sub>Cl<sub>2</sub>, –78°C, 2 h, 85–95%; h) **8** (1.15 equiv), TEA (1.25 equiv), MgSO<sub>4</sub>, CH<sub>2</sub>Cl<sub>2</sub>, RT, 1 h, then **7** (1.0 equiv), RT, overnight, 75–95%; i) **6** (1.0 equiv), **9** (1.0 equiv), AgOAc (0.1 equiv), TEA (1 equiv), CH<sub>3</sub>CN, RT, 5 h, 60–92%; j) 1 N DME/LiOH (5:3, aq), 0°C, 1–4 h, 82–95%; k) **10** (1.0 equiv), MeGly·HCl (1 equiv), DECP (1.2 equiv), DMF, 0°C, then TEA (2.0 equiv), RT, overnight, 64–95%; l) 1 N DME/LiOH (5:3, aq), 0°C, 1–4 h, 85–97%. DMP = 2,2-dimethoxypropane, Ts = *p*-toluenesulfonyl, DMF = *N,N*-dimethylformamide, DMSO = dimethylsulfoxide, DMP = 2,2-dimethoxypropane, TEA = triethylamine, DIPEA = diisopropylethylamine, DME = 1,2-dimethoxyethane, MeGly = glycine methyl ester, DECP = diethylcyanophosphonate.

stereocontrol when R<sup>3</sup> is a phenyl group, and R<sup>1</sup> = Me or Et (compounds **10a,c–e,g,i,j**). When R<sup>3</sup> is an alkyl group, the stereocontrol is variable and ranges from greater than 99:1 when R<sup>3</sup> = *t*Bu (**10b**) to 91:9 when R<sup>3</sup> = *c*Hex (**10f**) or *c*Pr (**10h**). In the case of pyrrolidine **10k**, which has a chiral group at R<sup>3</sup>, three stereoisomers were obtained in a ratio of 77:15:8.

Previous studies<sup>[6]</sup> have shown that the reaction between  $\pi$ -deficient alkenes and metalated azomethine ylides takes place through a stepwise mechanism, not a concerted

mechanism, to give the [3+2] cycloadduct. The first step comprises a Michael-type nucleophilic attack of the  $\alpha$  carbon atom of the azomethine ylide **A**, which forms in situ, on the  $\beta$  carbon atom of the nitroalkene (Scheme 2). The cyclization step takes place by means of an intramolecular Henry-type reaction between the intermediate nitronate moiety and the iminic fragment of the zwitterionic intermediate denoted as **B** in Scheme 2.



**Scheme 2.** Mechanism of formation of cycloadducts **10** from the reaction between imines **9** and nitroalkenes **6**. X<sub>c</sub><sup>+</sup> = chiral group.

To understand the origins of the stereocontrol of the reaction, we computed the two possible diastereomeric transition-state structures **TS1** and **TS1'** for the model system depicted in Figure 2.<sup>[7]</sup> As shown in Figure 2 and Scheme 2, part of the stereocontrol of the reaction stems from the retention of configuration of the *E*-nitroalkene and the

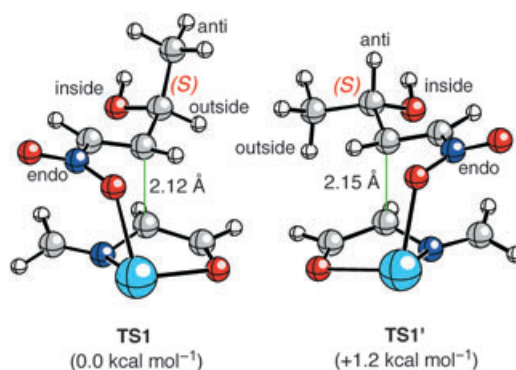


**Figure 2.** Ball-and-stick representations of the fully optimized structures of transition-state structures **TS1** and **TS1'** (C gray, O red, N dark blue, Ag light blue); green lines represent the new sigma bonds that form; see ref. [7] for further details.

chelated nature of the metalated azomethine ylide. The diastereoselectivity can be explained in terms of a two-electron interaction between the localized  $\sigma^*$  orbital of the C–C bond that forms and the localized  $\sigma$  orbital of the antiperiplanar C–CH<sub>3</sub> bond, with the alkoxy group occupying the inside position with respect to the pyrrolidine ring that forms, as seen in Figure 2. The alternative diastereomeric transition-state structure **TS1'**, in which the C–H bond is *anti* with respect to the new C–C bond that forms, is more than 1 kcal mol<sup>−1</sup> higher in energy than **TS1** and corresponds to high stereocontrol in favor of the (2*S*,3*R*,4*S*,5*S*) cycloadduct, provided that groups which are bulkier than methyl are used. The absolute configuration of the new stereogenic centers was verified by X-ray diffraction analysis on compound **11d** and confirmed the validity of our computational results.<sup>[8]</sup>

Next, the potential VLA-4 antagonism of compounds **11** was tested through a previously established model<sup>[2b]</sup> on VLA-4/VCAM-1-interaction-dependent B16M cell adhesion to primary cultured hepatic sinusoidal endothelial (HSE) cells in vitro. As shown in Figure 3, both B16M cell adhesion to TNF- $\alpha$  (tumor necrosis factor alpha)-treated HSE—which increases VCAM-1 expression on endothelial cells—and H<sub>2</sub>O<sub>2</sub>-treated B16M cell adhesion to unstimulated HSE cells—which increases VLA-4 activation in cancer cells—significantly increased relative to their respective untreated control cells ( $P < 0.01$ , where  $P$  is the statistical probability value).<sup>[2b]</sup> Preincubation of B16M cells with compounds **11** and measurement of adhesion to HSE resulted in variable responses as shown in Figure 3. Interestingly, compounds **11b** and **11h** with *t*Bu and *c*Pr groups at R<sup>3</sup>, respectively, did not show any significant antiadhesive activity. Similarly, compound **11e**, with a 2,6-difluorophenyl group at R<sup>2</sup> and a methyl group at R<sup>1</sup> was also almost inactive. In contrast, the presence of a quaternary atom at the  $\alpha$ -position of the pyrrolidine ring (R<sup>4</sup> = Me), such as in **11j**, did not result in a significant loss of activity.

To assess if interactions other than VLA-4/VCAM-1 were involved in the inhibitory activity of compounds **11**, we used the chemical shift perturbation method<sup>[9]</sup> on the I domain of the  $\alpha_2\beta_1$ -VLA-2 integrin which is also relevant in melanoma metastasis and binds different ligands such as collagen or laminin.<sup>[10]</sup> <sup>15</sup>N–<sup>1</sup>H heteronuclear single-quantum coherence (HSQC) NMR spectra<sup>[9]</sup> of uniformly <sup>15</sup>N-labeled I domain were recorded in the presence and the absence of inhibitors **11a–j**. In these spectra each amino acid of the I domain appeared as a cross-peak that corresponds to the NH group of its amide backbone. Analysis of the spectra at different pH values (pH 6.5 and 7.4) and at different temperatures ( $T = 283$  and  $298$  K, see Supporting Information) did not lead to any significant shift of the cross-signals upon addition of the inhibitors, which indicates the lack of binding and, therefore, the high selectivity of these compounds with respect to integrin VLA-2.

Although the best activity in vitro was shown by compound **11f**, which has a cyclohexyl group at R<sup>3</sup>, preliminary assays in vivo were carried out with **11d** (R<sup>3</sup> = Ph) because of its higher solubility in water. Additionally, **11d** displayed comparable antiadhesive activity to monoclonal antibodies against murine VLA-4 (Figure 3b). Furthermore,

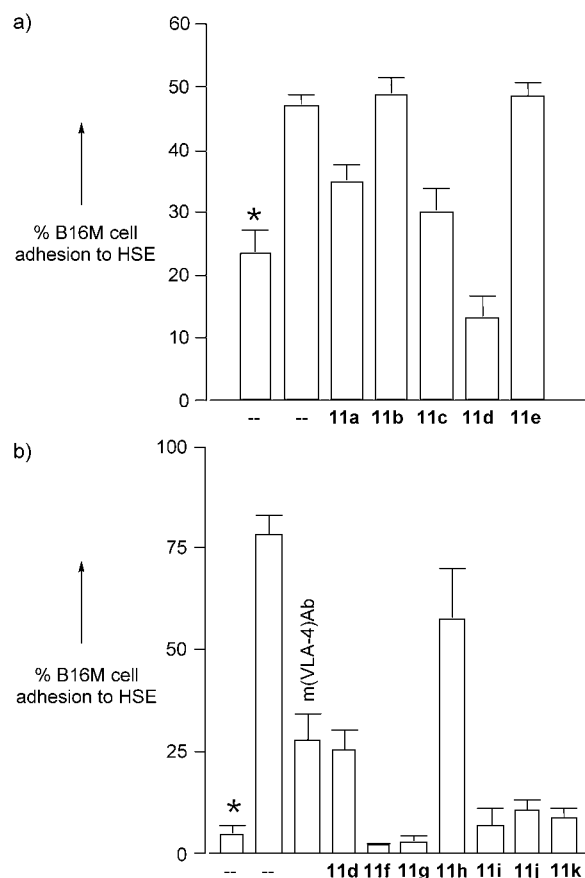


**Figure 3.** Inhibition of adhesion between HSE and B16M cells by compounds **11**. The degree of inhibition was measured on a) TNF- $\alpha$ -activated cultured HSE cells and b) H<sub>2</sub>O<sub>2</sub>-pretreated melanoma B16M cells. Asterisks (\*) indicate the inhibition measured on unstimulated HSE. The concentration of compounds **11** was 50  $\mu$ g per  $1 \times 10^6$  B16M cells. The lyophilized compounds were dissolved in DMSO and diluted to a final working stock solution of 5 mg mL<sup>−1</sup> in serum-free medium.  $1 \times 10^6$  B16M cells resuspended in 300  $\mu$ L of serum-free medium were preincubated with **11** (10  $\mu$ L of stock solution, 50  $\mu$ g) for 15 min at 37°C before the adhesion assay. m(VLA-4)Ab denotes rat anti-mouse CD49d monoclonal antibody (Serotec Ltd, Oxford, UK) against VLA-4. In this case, B16M cells were incubated with 10  $\mu$ g mL<sup>−1</sup> of m(VLA-4)Ab before the adhesion assay. The results are the mean standard deviation of three independent experiments, each performed in sextuplicate ( $n = 18$ ).

addition of **11d** compound to IL-1 $\beta$  (interleukin-1 $\beta$ )-treated melanoma cells completely abrogated their adhesion to immobilized VCAM-1 and prevented vascular endothelial growth factor (VEGF) production induced by soluble-VCAM-1-stimulated cells (see Supporting Information), which confirms the potent VLA-4 antagonism of compound **11d**. Finally, metastasis density and volume significantly decreased ( $P < 0.01$ ) by 60% and 95%, respectively, in mice that were intrasplenically injected with **11d**-pretreated B16M cells relative to those that received untreated cells (Figure 4). Parallel measurements on cell viability and cytotoxicity, intracellular oxidative metabolism, and cell-proliferation rates of **11d**-treated melanoma cells excluded that antimetastatic effects of **11d** compound may have been caused by



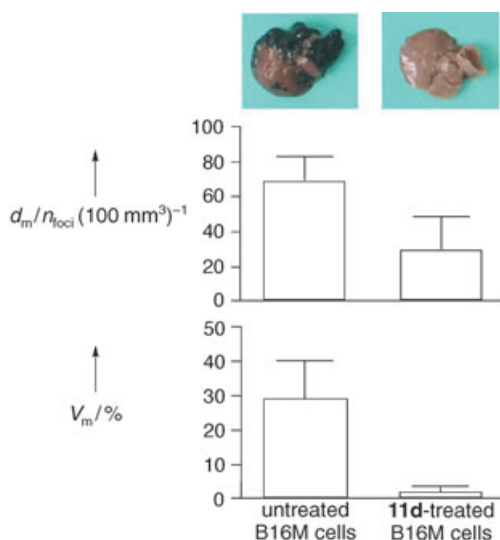


**Figure 4.** Antimetastatic activity of compound **11d** on male C57BL/6 mice (6 to 8 weeks old). At least 30 mice were used per experiment, and each experiment was carried out 3 times. The bars on the left correspond to the control group. The test group was treated with **11d**-pre-incubated B16M viable cells (50  $\mu$ g per  $1 \times 10^6$  B16M cells). Livers were removed on day 12 after intrasplenic injection of B16M cells and photographed. Photographs on the left and on the right correspond to livers obtained from the control and test groups, respectively. Metastases can be identified as black melanotic nodules. Metastasis density ( $d_m$ ) was measured as the number of foci per 100  $\text{mm}^3$  of liver, and metastasis volume ( $V_m$ ) was measured as the percentage fraction of liver volume occupied by metastases.

indirect effects on cell functions other than those specifically operated through a VLA-4-dependent mechanism.<sup>[11]</sup>

In summary, we have described a new family of inhibitors of the VLA-4/VCAM-1 interaction that 1) block the in vitro adhesion of melanoma cells to microvascular endothelium induced by proinflammatory cytokines and oxidative stress, 2) prevent melanoma cell production of VEGF induced by VCAM-1 in vitro, and 3) exhibit a potent antimetastatic activity in vivo. These small synthetic molecules fulfill the bioavailability requirements proposed by Lipinski et al.<sup>[12]</sup> Finally, the synthetic route developed for these inhibitors was convergent, completely regio- and stereoselective, versatile, and did not require sophisticated experimental devices or purifications. Therefore, it is well-suited to extensive studies of structural variation to refine the biological properties of the most promising lead compounds.

Received: November 2, 2004

Revised: February 14, 2005

Published online: April 13, 2005

**Keywords:** cell adhesion · cycloaddition · drug design · inhibitors · proteins

Reznikov, S.-H. Kim, Novick, M. Rubinstein, C. A. Dinarello, *Proc. Natl. Acad. Sci. USA* **2000**, *97*, 734.

- [3] For example, see: a) J. Boer, D. Gottschling, A. Schuster, B. Holzmann, H. Kessler, *Angew. Chem.* **2001**, *113*, 3988; *Angew. Chem. Int. Ed.* **2001**, *40*, 3870; b) S. Wattanasin, B. Weidmann, D. Roche, S. Myers, A. Xing, Q. Guo, M. Sabio, P. v. Matt, R. Hugo, S. Maida, P. Lake, M. Weetall, *Bioorg. Med. Chem. Lett.* **2001**, *11*, 2955; c) L. Chen, J. Tilley, R. v. Trilles, W. Yun, D. Fry, C. Cook, K. Rowan, V. Schwinge, R. Campbell, *Bioorg. Med. Chem. Lett.* **2002**, *12*, 137; d) G. A. Doherty, T. Kamenecka, E. McCauley, G. V. Riper, R. A. Mumford, S. Tong, W. K. Hagmann, *Bioorg. Med. Chem. Lett.* **2002**, *12*, 729; e) I. E. Kopka, D. N. Young, L. S. Lin, R. A. Mumford, P. A. Magriotis, M. MacCoss, S. G. Mills, G. V. Riper, E. McCauley, L. E. Egger, U. Kidambi, J. A. Schmidt, K. Lyons, R. Stearns, S. Vincent, A. Coletti, Z. Wang, S. Tong, J. Wang, S. Zheng, K. Owens, D. Levorse, W. K. Hagmann, *Bioorg. Med. Chem. Lett.* **2002**, *12*, 637; f) D. R. Leone, K. Giza, A. Gill, B. M. Dolinski, W. Yang, S. Perper, D. M. Scott, W.-C. Lee, M. Cornebise, K. Wortham, C. Nickerson-Nutter, L. L. Chen, D. Lepage, J. C. Spell, E. T. Whalley, R. C. Pether, S. P. Adams, R. R. Lobb, R. B. Pepinski, *J. Pharmacol. Exp. Ther.* **2003**, *305*, 1150.
- [4] For a related computational analysis of VCAM-1, see: A. Macchiarulo, G. Constantino, M. Meniconi, K. Pleban, G. Ecker, D. Bellocchi, R. Pellicciari, *J. Chem. Inf. Comput. Sci.* **2004**, *44*, 1829.
- [5] E. Y. Jones, K. Harlos, M. J. Bottomley, R. C. Robinson, P. C. Driscoll, R. M. Edwards, J. M. Clements, T. J. Dudgeon, D. I. Stuart, *Nature* **1995**, *373*, 539.
- [6] S. Vivanco, B. Lecea, A. Arrieta, P. Prieto, I. Morao, A. Linden, F. P. Cossio, *J. Am. Chem. Soc.* **2000**, *122*, 6078.
- [7] These calculations were performed at the B3LYP level of theory; see: a) A. D. Becke, *J. Chem. Phys.* **1993**, *98*, 5648; b) A. D. Becke, *Phys. Rev. A* **1988**, *38*, 3098; c) C. Lee, W. Yang, R. G. Parr, *Phys. Rev. B* **1980**, *37*, 785; d) S. H. Vosko, L. Wilk, M. Nusair, *Can. J. Phys.* **1980**, *58*, 1200. Carbon, nitrogen, oxygen, and hydrogen atoms were described by means of the 6-31G(d) basis set, whereas silver atoms were described by the Hay–Wadt effective core potential; see: P. J. Hay, W. R. Wadt, *J. Chem. Phys.* **1985**, *82*, 299. Harmonic analyses on **TS1** and **TS1'** showed that both saddle points have only one imaginary frequency associated with nuclear motion along the reaction coordinate associated with formation of a new C–C bond. Differences in energy include zero-point vibration energy corrections.
- [8] CCDC 252339 contains the supplementary crystallographic data for this paper. These data can be obtained free of charge from the Cambridge Crystallographic Data Centre via [www.ccdc.cam.ac.uk/data\\_request/cif](http://www.ccdc.cam.ac.uk/data_request/cif).
- [9] a) A. Bax, M. Ikura, L. E. Kay, D. A. Torchia, R. Tschudin, *J. Magn. Reson.* **1990**, *86*, 304; b) G. Bodenhausen, D. J. Buben, *Chem. Phys. Lett.* **1980**, *69*, 185.
- [10] a) R. Mortarini, A. Anichini, G. Parmiani, *Int. J. Cancer* **1991**, *47*, 551; b) D. Baronas-Lovell, J. L. Lauer-Fields, J. A. Borgia, G. F. Serrazza, M. Al-Ghoul, D. Minond, G. B. Fields, *J. Biol. Chem.* **2004**, *279*, 43503.
- [11] F. Vidal-Vanaclocha, L. Mendoza, N. Gallot, N. Telleria, F. P. Cossio, A. Zubia, E. Aldaba, unpublished results.
- [12] C. A. Lipinski, F. Lombardo, B. W. Dominy, P. J. Freaney, *Adv. Drug Delivery Rev.* **1997**, *23*, 3.

[1] a) I. J. Fidler, *Nat. Rev. Cancer* **2003**, *3*, 1; b) J. D. Hood, D. A. Cheresh, *Nat. Rev. Cancer* **2002**, *2*, 91.

[2] a) G. E. Rice, M. P. Bevilacqua, *Science* **1989**, *246*, 1303; b) F. Vidal-Vanaclocha, G. Fantuzzi, L. Mendoza, A. M. Fuentes, M. J. Anasagasti, J. Martín, T. Carrascal, P. Walsh, L. L.